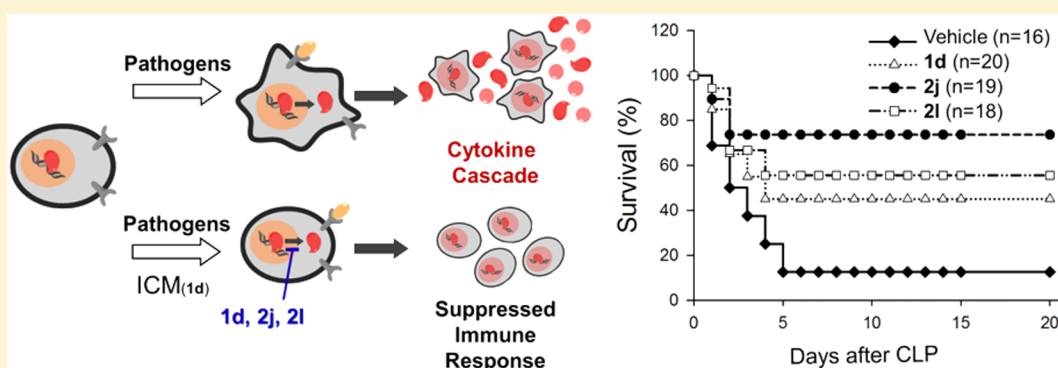


## Treatment of Sepsis Pathogenesis with High Mobility Group Box Protein 1-Regulating Anti-inflammatory Agents

Wansang Cho,<sup>†,‡,§</sup> Ja Young Koo,<sup>†,‡,§</sup> Yeonju Park,<sup>‡,§</sup> Keunhee Oh,<sup>§</sup> Sanghee Lee,<sup>†</sup> Jin-Sook Song,<sup>||</sup> Myung Ae Bae,<sup>||</sup> Donghyun Lim,<sup>⊥</sup> Dong-Sup Lee,<sup>‡</sup> and Seung Bum Park<sup>\*,†,⊥,||</sup><sup>†</sup>CRI Center for Chemical Proteomics, Department of Chemistry, Seoul National University, Seoul 08826, Korea<sup>‡</sup>Department of Biomedical Sciences, Seoul National University College of Medicine, Seoul 03080, Korea<sup>§</sup>Transplantation Research Institute, Seoul National University College of Medicine, Seoul 03080, Korea<sup>||</sup>Korea Bio-Organic Science Division, Korea Research Institute of Chemical Technology, Daejeon, 34114, Korea<sup>⊥</sup>Department of Biophysics and Chemical Biology, Seoul National University, Seoul 08826, Korea

## S Supporting Information



**ABSTRACT:** Sepsis is one of the major causes of death worldwide when associated with multiple organ failure. However, there is a critical lack of adequate sepsis therapies because of its diverse patterns of pathogenesis. The pro-inflammatory cytokine cascade mediates sepsis pathogenesis, and high mobility group box proteins (HMGBs) play an important role as late-stage cytokines. We previously reported the small-molecule modulator, inflachromene (**1d**), which inhibits the release of HMGBs and, thereby, reduces the production of pro-inflammatory cytokines. In this context, we intraperitoneally administered **1d** to a cecal ligation and puncture (CLP)-induced mouse model of sepsis and confirmed that it successfully ameliorated sepsis pathogenesis. On the basis of a structure–activity relationship study, we discovered new candidate compounds, **2j** and **2l**, with improved therapeutic efficacy in vivo. Therefore, our study clearly demonstrates that the regulation of HMGB1 release using small molecules is a promising strategy for the treatment of sepsis.

## INTRODUCTION

Sepsis, a systemic inflammatory response caused by infectious processes, is one of the major causes of death worldwide.<sup>1–3</sup> External pathogenic molecules known as pathogen-associated molecular patterns (PAMPs) are recognized by pattern recognition receptors (PRRs) in innate immune cells. The specific recognition of PAMP by the PRRs activates immune signaling, resulting in the production of various pro-inflammatory cytokines that mediate the inflammatory responses.<sup>4,5</sup> Sepsis occurs when immune responses are overactivated, including intractable inflammatory responses associated with imbalanced cytokine production. In addition, the subsequently unmanaged pro-inflammatory cytokine cascade results in whole body shock.<sup>1,6,7</sup> When the pathophysiology of sepsis is associated with hypoperfusion, hypotension, and organ dysfunction, it is termed as severe sepsis,<sup>1</sup> which occurs in approximately 10% of all intensive care unit patients

in the U.S.<sup>7–9</sup> Although numerous therapeutic approaches to sepsis have been advanced, the mortality rate of severe sepsis is nearly 20%.<sup>10</sup> Furthermore, the annual hospital healthcare cost for patients with severe sepsis in the U.S. is the highest among all diseases and was around \$20 billion.<sup>11</sup> The biggest obstacle to the discovery of therapeutics for sepsis is its diverse etiology among patients.<sup>12</sup> The heterogeneous patterns of sepsis pathogenesis depend on the pathogenic organisms and sites of infection.<sup>7,12</sup> The diverse characteristics of sepsis pathogenesis have prompted researchers to study the molecular mechanism of sepsis progression based on systemic inflammatory responses.

The emerging role of various pro-inflammatory cytokines in the progression of sepsis has been examined by a series of

Received: July 5, 2016

scientific studies.<sup>13–15</sup> Furthermore, tumor necrosis factor (TNF)- $\alpha$  and interleukin-(IL)-1 $\beta$  are two major pro-inflammatory cytokines involved in sepsis and their secretion is regulated by positive feedback during systemic inflammatory responses.<sup>15,16</sup> When the secreted cytokines circulate in the whole body, considerable amounts of cytokines are produced, resulting in septic shock and secondary multiple organ dysfunction.<sup>16</sup> Therefore, therapeutic approaches to antagonize the production of these cytokines have been used for the treatment of sepsis.<sup>17,18</sup> For example, an anti-TNF- $\alpha$  antibody underwent large-scale clinical trials but was discontinued because it lacked efficacy.<sup>7,19,20</sup> Literature reports suggest these failures might have been caused by two reasons. First, because the production of TNF- $\alpha$  and IL-1 $\beta$  peaks at the early stage of systemic inflammation, it is difficult to reverse the enhanced cytokine production without inhibiting the early stage of pathogenesis. Second, the continuous inflammatory stimuli unexpectedly restored the TNF- $\alpha$  levels after treatment with the antagonizing anti-TNF- $\alpha$  antibody.<sup>19–21</sup>

On the other hand, high mobility group box protein 1 (HMGB1) has been identified as a late-stage mediator of inflammatory responses.<sup>22</sup> HMGB1 is a DNA-binding protein that is associated with the nuclear genomic DNA. When damaged cells undergo necrotic death, HMGB1 is released into the extracellular milieu, alerting adjacent cells to the damage. Interestingly, in immune cells such as macrophages, HMGB1 is actively secreted as a pro-inflammatory cytokine during systemic inflammatory responses.<sup>23–26</sup> Previous reports have indicated that secreted HMGB1 plays an important role in regulating the production of other pro-inflammatory cytokines.<sup>27</sup> In this context, it has been reported that the inhibition of HMGB1 secretion successfully ameliorated the pathogenesis of sepsis in an in vivo cecal ligation and puncture (CLP) mouse model, the gold standard animal model in the field of sepsis study.<sup>28,29</sup> Briefly, the CLP mouse model is established by performing a surgical procedure to the cecum, which is the organ where the resident enteric microbiome exists. Ligating the cecum and puncturing the end with a needle causes endotoxemia by inducing polymicrobial contamination in the abdominal cavity toward the circulatory system. This action subsequently initiates a systemic inflammatory response, namely sepsis.

Regarding the role of HMGB1 in sepsis, Tracey and co-workers reported that the anti-HMGB1 antibody abrogated the lethality of the CLP-induced mouse model by inhibiting the release of HMGB1.<sup>30</sup> Endogenous small molecules such as cholinergic agonists have also inhibited HMGB1 secretion, thereby exhibiting the therapeutic effects in sepsis.<sup>31–33</sup> Furthermore, a known autophagy modulator, (–)-epigallocatechin-3-gallate (EGCG), has been studied for the prevention of lipopolysaccharide (LPS)-induced HMGB1 release by triggering the degradation of cytosolic HMGB1, thereby boosting the autophagic process.<sup>34–36</sup>

Previously, we reported the discovery of a novel small molecule, inflachromene (ICM, **1d**, Figure 1B), that inhibits the activation of BV-2 microglia-like cells, via screening a pDOS-based drug-like compound library.<sup>37,38</sup> On the basis of our efforts on target identification using the fluorescence difference in two-dimensional gel electrophoresis (FITGE) method,<sup>39</sup> we revealed HMGB1 and HMGB2 as the target proteins of ICM, and the subsequent biochemical and biophysical studies confirmed that ICM inhibits the secretion of HMGB1 and HMGB2 in microglia via the modulation of their post-

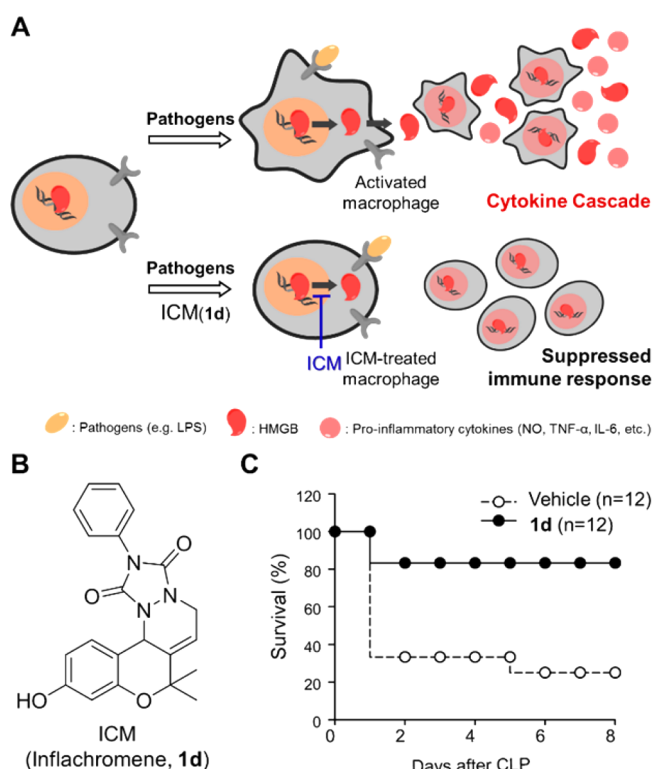


**Figure 1.** Structure and in vivo therapeutic effect of inflachromene (ICM, **1d**) in cecal ligation and puncture (CLP) model of sepsis. (A) During sepsis, the extracellular secretion of high-mobility group box protein 1 (HMGB1) occurs in activated macrophages. The small-molecule ICM (**1d**) inhibits the release of HMGB1, thereby suppressing immune responses. (B) Chemical structure of ICM. (C) Survival rate of vehicle- and ICM-treated CLP mouse model. ICM was administered intraperitoneally at a daily dose of 10 mg/kg for 9 days.

translational modifications.<sup>40</sup> On the basis of the fact that microglia in the central nervous system is a cell type sharing the same ontology with peripheral macrophages,<sup>41,42</sup> we hypothesized that ICM can inhibit the secretion of HMGB1 and HMGB2 in macrophages, reduce the production of additional pro-inflammatory cytokines, and thereby exhibit its therapeutic effect on the systemic inflammatory response. To test our hypothesis, we examined whether in vivo administration of ICM to CLP-induced mice inhibits sepsis pathogenesis by measuring the survival rate. On the basis of the initial proof-of-concept in vivo study, we investigated the enhancement of the anti-inflammatory efficacy of ICM in sepsis treatment by conducting a systematic structure–activity relationship study. After synthesizing approximately 30 ICM analogues, we examined their anti-inflammatory activities in Raw264.7 macrophage-like cells. Then, candidate compounds were selected based on a series of biological evaluations including the Griess assay, enzyme-linked immunosorbent assay (ELISA), microsomal stability testing, and pharmacokinetics (PK) as well as in vivo studies using a CLP mouse model. Finally, we discovered new candidate compounds with enhanced therapeutic efficacy against sepsis.

## RESULT AND DISCUSSION

**In Vivo Therapeutic Effect of ICM in CLP-Induced Mouse Model of Sepsis.** When pathogens invade a host organism, an acute inflammatory response is initiated in the body. Macrophages, one of the key immune cells that mediate

the inflammatory responses, are activated following their recognition of pathogens, which subsequently induces the secretion of various pro-inflammatory cytokines including HMGBs, TNF- $\alpha$ , and IL-6 (Figure 1A).<sup>4–6</sup> At the basal state, HMGBs are associated with genomic DNA within the nucleus. After activation of macrophage upon recognition of LPS, HMGBs are translocated from nucleus to cytosol and subsequently released to the extracellular milieu.<sup>43</sup> These pro-inflammatory cytokines activate other adjacent macrophages and initiate a positive feedback mechanism of immune response.<sup>44</sup> We previously reported that ICM (**1d**, Figure 1B) inhibits the translocation of HMGBs by blocking their post-translational modifications and subsequently reduces the secretion of HMGBs in microglia, which led to the suppression of neuroinflammatory response.<sup>40</sup>

Therefore, we envisaged that **1d** would be potentially efficacious for the treatment of sepsis. On the basis of this assumption, we adopted a murine CLP model, which is considered as the gold standard model of *in vivo* sepsis.<sup>28</sup> The intraperitoneal (ip) injection in the CLP-induced mice of 10 mg/kg of **1d** for 9 days significantly increased the survival rate compared to that of the vehicle-treated group (Figure 1C). The measurement of the serum cytokines after euthanizing the mice revealed that IL-6 levels were highly correlated with their survival (Supporting Information, Figure S1). Based on these data, we concluded that **1d** exhibited a potential therapeutic effect in sepsis.

**Synthesis and Biological Evaluation of ICM (1d) Analogues to Discover New Compounds with Enhanced Anti-inflammatory Effects.** To improve the therapeutic efficacy of **1d**, we first comprehensively explored the structure–activity relationship of its anti-inflammatory effects. Starting from the benzopyranyl core structure of **1d**, we designed and synthesized a series of analogues to clarify the importance of each structural motif. To measure the inhibitory effects on immune response, Raw264.7 cells were treated with the synthesized analogues in the presence of LPS, which is widely used to activate macrophages<sup>45</sup> because it is one of the major components of external membrane of Gram-negative bacteria.<sup>45–47</sup> LPS-activated macrophages produce various pro-inflammatory cytokines<sup>48,49</sup> and nitric oxide (NO), which was selected as the molecular marker to monitor the activation level of macrophages. We quantitatively measured the secreted NO level in the culture medium by using the Griess assay as an efficient high-throughput screening system.<sup>40,50</sup>

Our original hit compound (**1d**) inhibited the NO release by 87% in Raw264.7 cells compared to the vehicle. As shown in Table 1, the systematic modification of the R<sub>1</sub>, R<sub>2</sub>, R<sub>3</sub>, and R<sub>4</sub> groups of the benzopyranyl core structure revealed that most of R<sub>1</sub>, R<sub>2</sub>, and R<sub>3</sub> substituents (**1a–1h**) reduced the inhibition potency on NO release respect to **1d**: in particular substitution of the R<sub>2</sub> hydroxyl group with a methoxy one was very unfavorable. Even when both methyl groups of **1d** at the R<sub>4</sub> position were modified as in **1i–1j** analogues, the inhibition of cellular NO release was significantly reduced. These results indicate that the R<sub>1</sub>–R<sub>4</sub> groups' combination of **1d** is essential for the anti-inflammatory effects. Similarly, the shift or removal of the double bond of the tetrahydropyridazine ring failed to induce inhibitory effects on NO release (Supporting Information, Figure S2).

Next, we prepared a series of **1d** analogues by introducing various *N*-substituents of the tetracyclic benzopyranyl core, indicated as the R group in Table 2, via hetero-Diels–Alder

**Table 1. Relationship between Structural Modifications in Benzopyranyl Core and Percent (%) Inhibition of Released Nitric Oxide (NO) Level**

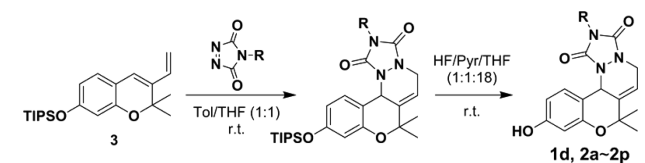
Cpd.	R <sub>1</sub>	R <sub>2</sub>	R <sub>3</sub>	R <sub>4</sub>	% NO inh. <sup>a</sup>
<b>1a</b>	H	H	H	methyl	83
<b>1b</b>	H	<i>N</i> -methylamino	H	methyl	52
<b>1c</b>	H	fluoro	H	methyl	79
<b>1d<sup>b</sup></b>	H	hydroxy	H	methyl	87
<b>1e</b>	H	methoxy	H	methyl	44
<b>1f</b>	methoxy	H	H	methyl	55
<b>1g</b>	methoxy	methoxy	H	methyl	44
<b>1h</b>	H	methoxy	hydroxy	methyl	26
<b>1i</b>	H	hydroxy	H		47
<b>1j</b>	H	hydroxy	H		36

<sup>a</sup>Percentage inhibition of NO by 10  $\mu$ M ICM and its analogues was measured in Raw264.7 cells by using Griess assay. <sup>b</sup>ICM, Cpd., compound; NO inh, nitric oxide inhibition.

reaction of the intermediate **3** with *N*-substituted 1,2,4-triazoline-3,5-diones. First, the replacement of the phenyl group of **1d** with a methyl one (**2a**) caused the lowest inhibitory effect (45%) on NO release, being reduced also with benzyl (**2b**) and cyclohexyl (**2c**) substitutions. Then we incorporated various substituents at the *ortho*, *meta*, and *para* positions of the original phenyl ring. The *ortho*-substituted compounds (**2d**, **2e**) exhibited little inhibitory effects on NO release. In contrast, a methoxy group at the *meta* (**2f**) and *para* (**2g**) positions enhanced the inhibition of NO release. To examine the relationship between the position of the methoxy group on the phenyl ring and the inhibition of NO release, we synthesized ICM analogues containing 3,4-(methylenedioxy)-phenyl (**2k**) and 3,5-dimethoxyphenyl (**2l**) as the R groups. A series of *para*-substituted (**2g–j**, **2m–o**) analogues were also synthesized, and their activity was evaluated by using the Griess assay. The screening results indicated that compounds **2g–2l** effectively inhibited the NO release compared to **1d** while **2m**, **2n**, and **2o** showed cytotoxicity at the higher concentration, which led us to discontinue their further biological evaluation. To confirm the anti-inflammatory activity of our synthesized compounds, we measured their inhibitory effect on the production of another cytokine, TNF- $\alpha$ . As shown in Table 2, compounds **1d** and **2f–2l** inhibited the TNF- $\alpha$  release in Raw264.7 cells. The amount of TNF- $\alpha$  released was quantitatively measured by using ELISA. On the basis of these results, we selected compounds **2i**, **2j**, **2k**, and **2l** as our improved candidate compounds for further biological evaluation.

**Inhibition of HMGB1 and IL-6 Release by Initial Hit Compounds.** For the secondary confirmation of biological activities, we first examined whether our initial hit compounds could inhibit the translocation of HMGB1. As mentioned

**Table 2. Effects of Structural Modifications Relative to the N-Substituents of the Triazolinedione Ring Structure of 1d on the Percentage (%) Inhibition of Nitric Oxide (NO) and Tumor Necrosis Factor (TNF)- $\alpha$  Release, As Well As on the Cell Viability (%)**



Cpd.	R	% NO inh. <sup>a</sup>	% viab. <sup>b</sup>	% TNF- $\alpha$ inh. <sup>c</sup>
1d <sup>d</sup>	phenyl	87	105	43
2a	methyl	45	114	<i>e</i>
2b	benzyl	70	106	<i>e</i>
2c	cyclohexyl	63	117	<i>e</i>
2d	2-iodophenyl	48	109	<i>e</i>
2e	2-methoxyphenyl	66	115	<i>e</i>
2f	3-methoxyphenyl	96	118	38
2g	4-methoxyphenyl	89	127	44
2h	4-fluorophenyl	87	109	44
2i	4-methylphenyl	94	130	45
2j	4-acetylphenyl	93	111	68
2k	3,4-(methylenedioxy)phenyl	92	121	46
2l	3,5-dimethoxyphenyl	94	121	60
2m	4-(trifluoromethyl)phenyl	85	106 <sup>f</sup>	
2n	4- <i>tert</i> -butylphenyl	99	105 <sup>f</sup>	
2o	4- <i>n</i> -butylphenyl	99	50 <sup>f</sup>	

<sup>a</sup>Inhibition of NO release (%) by each compound (10  $\mu$ M) was measured by using Griess assay in Raw264.7 cells. Cpd., compound; WST, water-soluble tetrazolium; ELISA, enzyme-linked immunosorbent assay. <sup>b</sup>Relative cell viability (%) of each compound (10  $\mu$ M) in the presence of LPS was measured by using WST assay, and compared to vehicle. <sup>c</sup>Inhibition of TNF- $\alpha$  release (%) by each compound (10  $\mu$ M) was measured by using ELISA. <sup>d</sup>ICM. <sup>e</sup>Excluded by low NO inhibition (%). <sup>f</sup>Excluded due to the cellular toxicity observed at the higher concentration.

earlier, HMGBs are translocated from the nucleus to cytosol in activated macrophage before they are released into the extracellular milieu. Therefore, we measured the cellular localization of HMGB1 upon LPS treatment in the absence and presence of our hit compounds using immunohistochemistry (TRITC-labeled secondary antibody). As shown in Figure 2A, our initial hit compounds (2i, 2j, 2k, 2l, and 1d) inhibited the translocation of HMGB1 from the nucleus to the cytosol induced by LPS-treatment. Because we observed a drastic decrease of IL-6 levels in the surviving CLP-induced mice treated with 1d (Supporting Information, Figure S1), we measured the secreted IL-6 levels in Raw264.7 cells. The Western blot analysis confirmed that the secreted IL-6 levels were significantly decreased upon treatment with 1d, 2i, 2j, 2k, and 2l in LPS-activated macrophages (Figure 2B). Interestingly, we also observed the reduction of intracellular IL-6 levels upon treatment with hit compounds, which indicates that the positive feedback of cytokine production was inhibited by our molecules. Furthermore, among the initial hit compounds, 2j and 2l showed superior inhibitory efficacy on IL-6 secretion (Figure 2B) and TNF- $\alpha$  release (Table 2).

To confirm the improved activity of 2j and 2l, we performed in vitro binding competition assay using ICM-BP (Figure 2C). ICM-BP has a photoactivatable benzophenone moiety for

covalent UV cross-linking with adjacent proteins and a bioorthogonal alkyne moiety for fluorophore conjugation via click reaction.<sup>39</sup> We previously used ICM-BP for the identification of HMGBs as the target protein of 1d and demonstrated its competitive binding toward HMGBs with 1d in the cellular system.<sup>40</sup> With this ICM-BP in hand, we evaluated the relative binding affinity of candidate compounds 1d, 2j, or 2l with HMGB1 by comparing the competitive labeling of fluorophores toward HMGB1 (Figure 2D). As shown in Figure 2E, we clearly observed the reduced labeling of Cy5 in the presence of either 1d, 2j, or 2l in a dose-dependent manner. But the negative compound 2a did not show any dose-dependent competition, which confirms the specific competitive binding event of ICM-BP with candidate compounds. On the basis of this experiment, we could confirm that 2j and 2l might bind more tightly than 1d, which suggests that 2j and 2l might have enhanced activities in the regulation of HMGB1. Moreover, on the basis of our preliminary docking simulation with HMGB1, 2j and 2l showed lower binding energies to HMGB1 than the original ligand 1d did (Supporting Information, Figure S3). Therefore, we selected 2j and 2l as candidate compounds with enhanced anti-inflammatory effect for further in vivo evaluation.

**Inhibition of Inflammatory Signaling Pathway by Candidate Compounds (1d, 2j, and 2l).** Intracellular inflammatory signaling pathways play important roles in propagating immune responses in the activated macrophage. Mitogen-activated protein kinase (MAPK) and nuclear factor kappa-light-chain enhancer in B cells (NF- $\kappa$ B) complex are two of the most important inflammatory signaling systems that regulate the release of HMGBs and other cytokines in macrophages.<sup>4,51,52</sup> There are three distinct types of MAPKs: p38 MAPK (p38), c-jun N-terminal kinases (JNKs), and extracellular signal-regulated kinase (ERK). Following the activation of macrophage, the MAPKs are phosphorylated and subsequently trigger the transduction of inflammatory signals within the cells.<sup>52,53</sup> The Western blot data showed that our compounds 1d, 2j, and 2l clearly inhibited the phosphorylation of MAPK including p38, JNK, and ERK (Figure 3A,B).

The NF- $\kappa$ B pathway is another key signaling pathway that regulates inflammatory responses. NF- $\kappa$ B is a complex of two different protein domains, p50 and p65. In the basal state, the activity of the NF- $\kappa$ B complex is inhibited by nuclear factor of kappa-light polypeptide gene enhancer in B-cells inhibitor (I $\kappa$ B). When the activation signal reaches the macrophages, I $\kappa$ B kinase (IKK) phosphorylates I $\kappa$ B, which is subsequently degraded leading to the activation of the NF- $\kappa$ B complex. The activated NF- $\kappa$ B then translocates to the nucleus and acts as a transcription factor to produce pro-inflammatory cytokines. In this signaling pathway, the cellular translocation of the NF- $\kappa$ B complex is the key event in the activation of the macrophages.<sup>51,54</sup> As expected, the nuclear translocation of the NF- $\kappa$ B was inhibited by treatment with our candidate compounds 1d, 2j, and 2l, as evidenced by immunofluorescence assays on p65 subunit (Figure 3C and Supporting Information, Figure S5). On the basis of these observations, we concluded that our candidate compounds 1d, 2j, and 2l regulated the inflammatory signaling pathways in activated macrophages.

#### Pharmacokinetics of ICM and Selected Compounds.

Before investigating the selected compounds, 1d, 2j, and 2l in the in vivo CLP-induced mouse model, we measured their

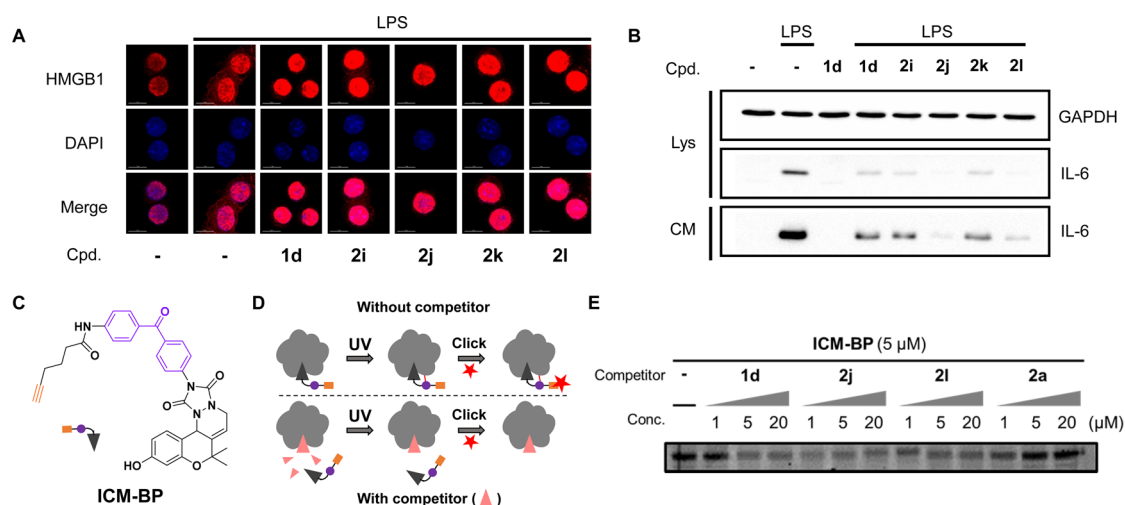


**Figure 2.** Inhibition of high mobility group box protein B1 (HMGB1) translocation and interleukin (IL)-6 release upon treatment with **1d**, **2i**, **2j**, **2k**, and **2l**. (A) Cellular immunofluorescence images of HMGB1 after pretreatment with  $20\ \mu\text{M}$  of **1d**, **2i**, **2j**, **2k**, and **2l** for 1 h, followed by  $500\ \text{ng/mL}$  lipopolysaccharide (LPS) treatment. Dimethyl sulfoxide (DMSO) was the control. (B) Western blot analysis of released IL-6 after pretreatment with  $10\ \mu\text{M}$  of **1d**, **2i**, **2j**, **2k**, and **2l** for 1 h, followed by  $100\ \text{ng/mL}$  LPS treatment of Raw264.7 cells. Images shown represent at least three independent experiments. (C) Structure of ICM-BP. Purple, benzophenone moiety; orange, alkyne moiety. (D) Schematic figure of in vitro binding competition assay. After UV cross-linking of ICM-BP, Cy5-azide was incorporated via bioorthogonal click reaction. (E) Fluorescence gel image of purified HMGB1 protein labeled with Cy5-azide. The same amount of HMGB1 was loaded into each lane. Competitor **1d**, **2j**, and **2l** were treated to the purified HMGB1 protein in a dose-dependent manner prior to the treatment of ICM-BP ( $5\ \mu\text{M}$ ). **2a** was treated as a negative control, of which data exhibit no dose-dependency. Cpd., compound; Lys, cell lysate; CM, culture medium; Conc., concentration.

aqueous solubility,<sup>55</sup> liver microsomal stabilities, and PK profiles (Table 3). Compared to **1d**, compounds **2j** and **2l** showed improved solubility in aqueous media and improved liver microsomal stability in both mice and humans. Probably, the PK data revealed that although the area under the curve (AUC) values of **2j** and **2l** were lower than that of **1d**, their comparable (**2j**) or longer (**2l**) half-life was expected to contribute to a better efficacy in the in vivo sepsis model. The **1d**, **2j**, and **2l** were all easily administered by ip injection and retained their activities for several hours. Along with their biological activities found in previous biological experiments, these results indicate that the compounds **1d**, **2j**, and **2l** all performed adequately in the in vivo mouse model following ip administration.

**Enhanced in Vivo Therapeutic Effect of **2j** and **2l** in CLP-Induced Mouse Model of Sepsis.** Finally, we compared the in vivo therapeutic effect of **1d**, **2j**, and **2l** in a CLP-induced mouse model. The surgical procedure used to perform the CLP is illustrated in Figure 4A. Briefly, after excising the abdomen, the exposed cecum was ligated just below the ileocecal valve and then punctured using a surgical needle. Then, the excised abdomen was closed. The CLP-induced mice were treated with our candidate compounds for 21 days by daily ip injection, observing that the survival rate of the **1d**-, **2j**-, and **2l**-treated mice was significantly improved compared to that of the vehicle-treated mice (Figure 4B). Compared to **1d** with a 45% survival rate, 74% and 56% were found for **2j**- and **2l**-treated mice, respectively, while only 10% of the vehicle-treated mice survived. Furthermore, serum IL-6 levels were significantly decreased in the survived mice (Supporting Information, Figure S6), which is consistent with our previous observation in Figure 2B and Supporting Information, Figure S1. Therefore, we successfully enhanced the therapeutic effect of **1d** by structural optimization obtaining **2j** and **2l** as potential drug candidates for the treatment of sepsis.

## CONCLUSION

In this study, we explored the therapeutic efficacy in the treatment of sepsis of a previously reported small molecule, ICM (**1d**), which regulated the secretion of HMGB1 and HMGB2 in activated microglia.<sup>40</sup> Pro-inflammatory cytokines, such as TNF- $\alpha$  and IL- $1\beta$ , have shown limited clinical usefulness because of their characteristic early stage mediator effects,<sup>7,19–21</sup> while the clinical relevance of antagonizing HMGBs in sepsis has been proposed and reported in several studies.<sup>30–36</sup> Indeed, as late-stage mediators of systemic inflammatory responses, HMGBs regulate the production of other pro-inflammatory cytokines, thereby modulating the systemic inflammatory response. Therefore, the inhibition of HMGB1 release could downregulate the production of pro-inflammatory cytokines.<sup>30,31</sup> With this in mind, we evaluated our novel HMGB1-regulating compound, ICM (**1d**), in an in vivo CLP-induced mouse model, finding that it efficiently ameliorated the sepsis pathogenesis.

We further sought to improve the efficacy of **1d** by synthesizing 30 analogues, and their anti-inflammatory activities were evaluated by monitoring the inhibition of NO release in the Griess assay. On the basis of our structure–activity relationship study and secondary biological evaluations, we selected **2j** and **2l**, with different substituents on the **1d** phenyl ring, as our final candidates. Both **2j** and **2l** inhibited the translocation of HMGB1 from the nucleus to the cytosol, improved the inhibition of IL-6 release, and regulated the downstream inflammatory signaling pathways. Furthermore, **2j** and **2l** also showed better liver microsomal stabilities and reasonable PK profiles compared to that of **1d**. Finally, the daily ip administration of **2j** and **2l** in the in vivo CLP-induced mouse model showed enhanced therapeutic effects and **2j** exhibited the best therapeutic efficacy against sepsis. Therefore, this research study has provided considerable evidence supporting the use of selective regulation of HMGB1 release

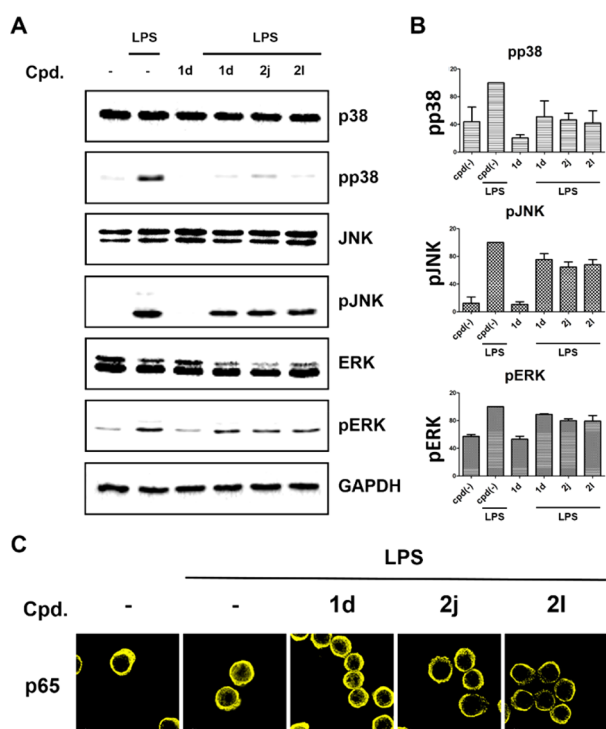


**Figure 3.** Inhibition of inflammatory signaling pathways in Raw264.7 cells. (A) Western blot analysis relative to the phosphorylation (p) of p38, JNK, and ERK after pretreatment with 20  $\mu\text{M}$  1d, 2j, or 2l in Raw264.7 cells, followed by 100 ng/mL LPS treatment. DMSO was the control. (B) Quantification of phosphorylation level of p38, JNK, and ERK after compound treatment by Western blot analysis. (C) Cellular NF- $\kappa$ B p65 immunofluorescence images after pretreatment with 20  $\mu\text{M}$  1d, 2j, or 2l in Raw264.7 cells, followed by 500 ng/mL LPS treatment. Data represent at least three independent experiments. Cpd., compound; GAPDH, glyceraldehyde 3-phosphate dehydrogenase; LPS, lipopolysaccharide; DMSO, dimethyl sulfoxide; pERK, phosphorylated extracellular signal-regulated kinase; pJNK, phosphorylated c-Jun N-terminal kinase; pp38, phosphorylated p38; NF- $\kappa$ B, nuclear factor kappa-light chain enhancer in B cells.

as a promising therapeutic strategy for the treatment of sepsis by using small molecules.

## EXPERIMENTAL SECTION

**Cell Culture.** Raw264.7 macrophage cell was cultured in Dulbecco Modified Eagle Medium (DMEM) with 10% (v/v) fetal bovine serum (FBS) and 1% (v/v) antibiotic-antimycotic solution. Cell was maintained in a 100 mm cell culture dish, in a 5%  $\text{CO}_2$  incubator at 37  $^\circ\text{C}$  with humidified atmosphere.

**Griess Assay and WST Assay.** Griess assay reagent was generated prior to the assay with the following contents listed below: *N*-(1-naphthyl)ethylenediamine dihydrochloride, 0.1% (m/v); sulfanilamide, 1% (m/v); phosphoric acid (85%), 5% (v/v) in deionized water. Raw264.7 cell was seeded in transparent 96-well plate and maintained for 1 day. Media was aspirated, and each well was washed with serum-free DMEM for twice. Each well was refilled with serum-free DMEM. Then 100 ng/mL LPS and compounds were treated after ward and cultured for 24 h. After the incubation, the supernatant culture media was transferred to new 96-well plate and mixed with 50  $\mu\text{L}$  of Griess assay reagent. Blank values were measure by mixing 50  $\mu\text{L}$  of Griess assay reagent with 10% FBS and 1% antibiotic-antimycotic containing DMEM. Four wells each were used for the control experiment, LPS and DMSO (without any compounds) treated well, and DMSO-only treated well. Without LPS, Raw264.7 cell does not release the nitric oxide in measurable concentration. Cell-seeded plate was conserved for further WST assay. Media-reagent mixture was incubated at room temperature for several minutes. Absorbance was read at 548 nm. Immediately after transferring media, cell-seeded wells were refilled with 100  $\mu\text{L}$  of 10% FBS and 1% antibiotic-antimycotic containing DMEM. Then 10  $\mu\text{L}$  of Ez-cytox WST assay reagent was used to treat each well, following the manufacturer's protocol. After incubating 20 min in a 5%  $\text{CO}_2$  incubator at 37  $^\circ\text{C}$  with humidified atmosphere, absorbance was read at 450 nm. Blank values were obtained from the well only treated with 10% FBS and 1% antibiotic-antimycotic containing DMEM. All experiments were independently performed at least three times.

**ELISA Assay.** For the quantification of secreted TNF- $\alpha$ , Raw264.7 cell was seeded in transparent 96-well plate and maintained for 1 day. Media was aspirated after 1 day and replaced to serum-free DMEM with 1% (v/v) antibiotic-antimycotic solution. LPS and compounds were treated in a final concentration of 100 ng/mL and 10  $\mu\text{M}$ . After 4 h, media were transferred to new transparent 96-well plate and diluted with 1% BSA in PBS solution. ELISA assay was performed following the manufacturer's protocol. Standard curve was plotted by the dose-dependent treatment of the control TNF- $\alpha$  protein provided with the ELISA kit. Blank value was measured by adding solutions without TNF- $\alpha$  substrate. All experiments were independently performed at least three times.

For the quantification of serum IL-6 level in CLP-induced C57BL/6 mice, blood was collected from mice at 24 h after surgery. ELISA plates (Costar, Cambridge, MA) were coated overnight with anti-IL-6 monoclonal antibody (eBioscience, San Diego, CA) at 4  $^\circ\text{C}$ . Wells were blocked with PBS containing 1% bovine serum albumin (Sigma-Aldrich, St. Louis, MO) for 1 h at room temperature (RT) and incubated with serum overnight at 4  $^\circ\text{C}$ . After washing, plates were incubated with biotinylated anti-IL-6 antibody (eBioscience) for 1 h at RT, followed by streptavidin-conjugated horseradish peroxidase (eBioscience) for 1 h at RT. Color was developed using TMB solution (eBioscience), and absorbance was read at 450 nm with a Multiskan Ascent (Labsystems, Kennett Square, PA). All assays were performed in triplicate and were independently repeated three times.

**Table 3.** Aqueous Solubility, Liver Microsomal Stability, and Pharmacokinetic (PK) Data of 1d, 2j, and 2l<sup>a</sup>

Cpd.		1d	2j	2l
solubility	aqueous ( $\mu\text{g}/\text{mL}$ )	23.5 $\pm$ 1.02	162.5 $\pm$ 2.12	65.1 $\pm$ 2.74
microsomal stability	mouse (%)	0.41 $\pm$ 0.10	2.46 $\pm$ 1.83	20.2 $\pm$ 1.78
	human (%)	0.82 $\pm$ 0.29	30.2 $\pm$ 2.81	41.2 $\pm$ 4.33
PK data	$T_{\text{max}}$ (h)	0.14 $\pm$ 0.10	0.25 $\pm$ 0.00	0.14 $\pm$ 0.10
	$C_{\text{max}}$ ( $\mu\text{g}/\text{mL}$ )	387 $\pm$ 122	100 $\pm$ 3.72	282 $\pm$ 87.0
	AUC ( $\mu\text{g}/\text{mL}\cdot\text{h}$ )	327 $\pm$ 68.7	202 $\pm$ 28.1	218 $\pm$ 51.8
	$T_{1/2}$ (h)	3.87 $\pm$ 0.84	3.45 $\pm$ 1.00	5.00 $\pm$ 0.98

<sup>a</sup>Equilibrium aqueous solubility of 1d, 2j, and 2l was measured by  $\mu\text{sol}$  method. PK data were obtained after 10 mg/kg of each compound was administrated by intraperitoneal (ip) injection. Among PK parameters,  $C_{\text{max}}$ ,  $T_{\text{max}}$ , AUC, and  $T_{1/2}$  were measured. Liver microsomal stability was measured by quantifying percentage remaining compound after 30 min. Data are means  $\pm$  standard deviation (SD,  $n = 3$ ).  $C_{\text{max}}$ , maximum concentration;  $T_{\text{max}}$ , time to achieve  $C_{\text{max}}$ ; AUC, area under the curve;  $T_{1/2}$ , half-life.

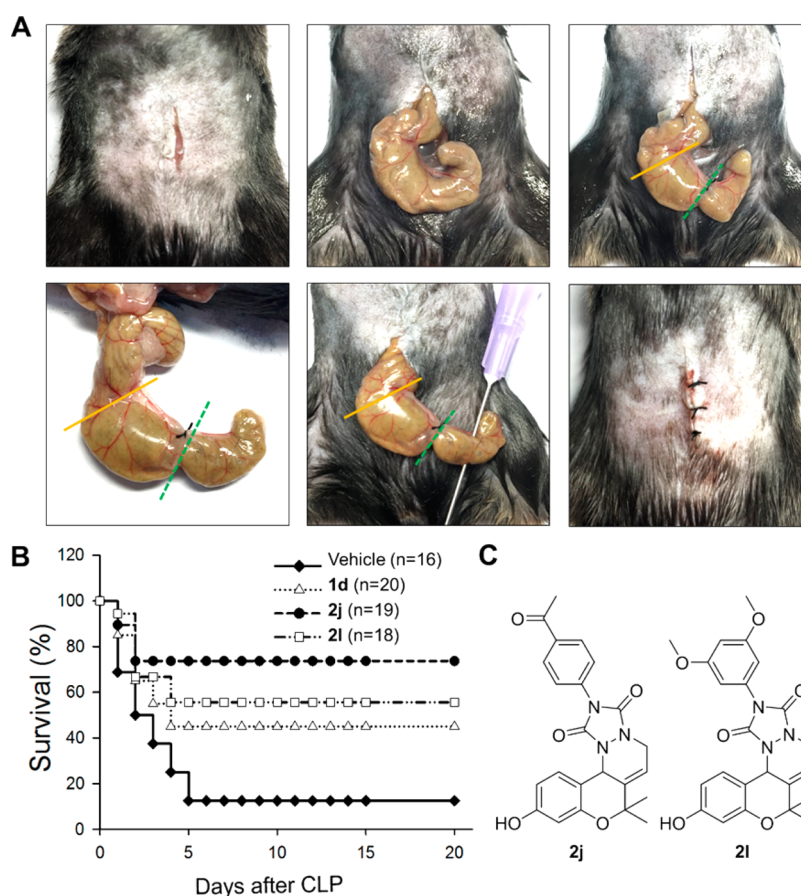


**Figure 4.** Therapeutic effect of selected compounds in in vivo CLP-induced mouse model. (A) Cecal Ligation and puncture procedure. Severity of sepsis can be controlled by the position of ligation. (B) Percentage survival rate of vehicle- and compound **1d**-, **2j**-, and **2l**-treated CLP-induced mice. **1d**, **2j**, and **2l** were administered intraperitoneally in a daily dose of 10 mg/kg for 21 days, starting from 1 h prior to CLP induction. Data shown is the accumulation of three independent experiments, each trial with at least  $N = 5$ . (C) Chemical structure of **2j** and **2l**.

**Western Blot.** Protein sampling was done in 4 °C. Cells were harvested in RIPA lysis buffer containing protease inhibitor cocktail and phosphatase inhibitor. After centrifugation at 15000 rpm for 20 min, supernatant was transferred to new 1.5 mL tube. Protein concentration was normalized with a Micro BCA protein assay kit. Prepared protein samples were analyzed with SDS-PAGE and following Western blot procedure. Protein was transferred into PVDF membrane after SDS-PAGE. Membrane was blocked after transfer step, with 2% BSA in TBST for 1 h in room temperature. Primary antibodies were treated overnight at 4 °C or 1 h in room temperature, followed by washing with TBST. HRP-conjugated secondary antibodies were treated for 1 h in room temperature. Antibodies were diluted in 1% BSA in TBST solution, with the concentration indicated in antibody manufacturer's protocol. After washing with TBST, membrane was developed by Amersham ECL prime solution. Chemiluminescent signal was measured by ChemiDoc MP imaging system, and relative quantification were followed using ImageLab 4.0 software. Quantification result was processed with GraphPad Prism 5.0 software.

**Immunofluorescence.** Raw264.7 cell was seeded in Nunc Lab-Tek II chambered coverglass and maintained for 1 day. Then 20  $\mu$ M of compounds were treated 1 h prior to 500 ng/mL LPS treatment for 2 h. After aspirating the media and washing with PBS, 200  $\mu$ L of 4% paraformaldehyde solution was treated and incubated at room temperature for 20 min. Then 4% paraformaldehyde solution was aspirated and the sample was washed with PBS three times. For the permeabilization to enable antibody binding, 200  $\mu$ L of methanol was treated and incubated at -20 °C for 20 min. Methanol was then removed and the sample was washed with PBS three times. Sample was blocked with 2% BSA in PBS solution at room temperature for 1

h. Then 2% BSA in PBS solution was removed and primary antibody containing 1% BSA in PBS was treated at 4 °C overnight. Antibody concentration was optimized according to the manufacturer's protocol. Primary antibody solution was removed and sample was washed with PBS three times. Secondary antibody containing 1% BSA in PBS solution was treated at room temperature for 1 h. The secondary antibody used was goat antirabbit TRITC labeled antibody from Abcam. After 1 h, antibody solution was aspirated and the sample was washed with PBS three times. For nucleus staining, Hoechst 33342 was diluted in PBS, and each well was treated and incubated at room temperature for 1 h. Hoechst 33342 was then removed and the chamber was filled with PBS, continued for imaging using DeltaVision microscope.

**DeltaVision Imaging.** DeltaVision Elite imaging system was used for the immunofluorescence imaging of HMGB1 and p65 translocation in Raw264.7 cell. Chamber was maintained with constant temperature of 25 °C. Image was obtained with 60 $\times$  scale, using DAPI/DAPI and TRITC/TRITC filter set: DAPI (excitation, 390/18 nm; emission, 435/48 nm), and TRITC (excitation, 542/27 nm; emission, 597/45 nm). Images were analyzed and merged with SoftWorks deconvolution software.

**In Vitro Fluorescence Binding Competition Assay.** Purified HMGB1 protein from R&D Biosystems were reconstituted in deionized water. Then 1  $\mu$ g of HMGB1 solution was transferred to a 20  $\mu$ L PCR tube (Axygen). Compounds were diluted in deionized water from 20 mM DMSO stock solution. The final concentration of DMSO was adjusted to 0.8%. Diluted competitors were pretreated for 60 min, and then ICM-BP was treated for additional 20 min. After compound treatment, 365 nm UV light from BLAK-Ray (B-100AP) UV lamp (UVP, USA) was irradiated to each sample for 5 min on ice.

The samples were then subject to click reaction with Cy5-azide (Lumiprobe, USA) (40  $\mu$ M) in the solution of tris[(1-benzyl-1*H*-1,2,3-triazol-4-yl)methyl]amine (TBTA) (Sigma, USA) (100  $\mu$ M), CuSO<sub>4</sub> (Sigma, USA) (1 mM), tris(2-carboxyethyl)phosphine (TCEP) (TCI, Japan) (1 mM), and tBuOH (Sigma, USA) (5%) for 90 min. Then 5× Lammeli buffer was added to the sample and incubated for 5 min at room temperature. Samples were loaded in 12.5% polyacrylamide gel for 1D gel electrophoresis. Finally, fluorescence was scanned by Typhoon Trio (Amersham Bioscience, USA).

**Computational Calculation.** Prior to the docking simulation study, the conformers of each ligand were generated by V<sub>conf</sub>2.0 using Tork conformational analysis method.<sup>56</sup> The binding modes and binding energies of ICM-derived ligands in HMGB1 were predicted by docking simulation using the Discovery Studio 1.7 program. Prediction of binding modes were calculated from cavities in X-ray crystal structure of HMGB1 (PDB 1HMF). Graphical analyses were performed with UCSF Chimera package version 1.8. Chimera developed by the Resource for Biocomputing, Visualization, and Informatics at the University of California, San Francisco.

**Liver Microsomal Stability and Pharmacokinetics.** Liver metabolic stability of compounds was examined in both mouse and human liver microsomes. Compounds were mixed with mouse or human liver microsomes (Gentest, BD Biosciences) in 100 mM potassium phosphate buffer (pH 7.4) and incubated at 37 °C for 5 min. Initiation of reaction was done by NADPH regeneration solution (BD Biosciences), and termination was performed by adding ice-cold acetonitrile (three times volume), with imipramine (80 ng/mL) as an internal standard at single time-point 30 min. After pretreating the biological samples with vortex and centrifuge, samples were analyzed by LC/MS/MS system. Pharmacokinetic data was obtained by following procedure. The candidate compound **1d**, **2j**, and **2l** were administered by ip injection (10 mg/kg) in ICR male mice (*n* = 5). **1d**, **2j**, and **2l** were prepared as a solution (DMSO, PEG400, and distilled water at 5:40:55, v:v:v %). Blood samples were taken at 10 and 30 min and at 1, 4, 8, and 24 h after injection. After the centrifugation of plasma for purification, the concentrations of candidate compound **1d**, **2j**, and **2l** were analyzed using Agilent 6460 LC/MS/MS system (Agilent) using electron spray ionization and a reverse-phase column (Hypersil GOLD C18, 50 mm × 2.1 mm, Thermo Scientific). Pharmacokinetic parameters were obtained after the analysis of plasma concentration–time plot with WinNonlin software (Pharsight).

**Mice and Cecal Ligation and Puncture (CLP) Experiments.** C57BL/6 (B6) mice were obtained from The Jackson Laboratory (Bar Harbor, ME). All mice were bred and maintained in specific pathogen-free conditions at the animal facility of Seoul National University College of Medicine. All animal experiments were performed with the approval of the Institutional Animal Care and Use Committee (IACUC) at Seoul National University (authorization no. SNU05050203). For CLP induction, after anesthesia, a 15 mm midline incision was performed in the abdomen to expose the cecum. The exposed cecum was ligated with 6–0 prolene just below the ileocecal valve (5.0 mm from the cecal tip). The cecal stump was punctured once with a 20-gauge needle, and small amount of stool (1 mm) was extruded. The cecum was placed back into its normal intra-abdominal position, and the abdomen was closed with a running suture of 6–0 prolene. Mice were treated with candidate compounds for a daily dose of 10 mg/kg/day for 21 days by intraperitoneal injection, starting from 1 h prior to CLP induction.

**Purity Determination from HPLC Analysis.** Reverse-phase HPLC analysis was performed with VP-ODS C-18 column (150 mm × 4.6 mm) at a flow rate of 1.0 mL/min. This HPLC system was equipped with a Shimadzu LC-6AD pump and a SPD-10A detector (Japan). HPLC solvents consist of water containing 0.1% trifluoroacetic acid (TFA) (solvent A) and acetonitrile containing 0.1% TFA (solvent B). Solvent A:B ratio was gradually increased, from 5:95 to 100:0 for 30 min, then 100:0 for at least 15 min. HPLC spectra were obtained based on the absorption wavelengths of 210 and 254 nm for the confirmation of ≥95% purity based on the area percentage. HPLC spectra and purity values of **2e**, **2j**, **2k**, **2l**, **2m**, and **2o** are in the Supporting Information.

**Preparation of Compounds 1a–j, 2a–o.** Preparation and characterization of all new compounds (**2e**, **2j**, **2k**, **2l**, **2m**, and **2o**) were described. Preparation and characterization of **1a–j**, **2a–d**, **2f–i**, **2n**, and diene-intermediate **3** were previously reported.<sup>57</sup>

**Detailed Synthetic Procedure for the Preparation of 2e, 2j, 2k, 2l, 2m, and 2o.** To a solution of **3** (0.9 mmol) in anhydrous toluene (5 mL), a red-colored solution of appropriate 4-substituted-1,2,4-triazoline-3,5-dione (1.5 equiv) in THF (5 mL) was added. (Preparation of appropriate 4-substituted-1,2,4-triazoline-3,5-dione was previously reported.<sup>54</sup>) The reaction mixture was stirred at room temperature for 1 to 6 h until the complete consumption of starting material **3**. After the reaction completion monitored by TLC, the resulting mixture was concentrated in vacuo and purified with silica-gel flash column chromatography to provide the desired product, TIPS-protected ICM derivative. Yields: 59%, TIPS-**2e**; 44%, TIPS-**2j**; 41%, TIPS-**2k**; 49%, TIPS-**2l**; 35%, TIPS-**2m**; 73%, TIPS-**2o**.

Finally, the resulting TIPS-protected ICM derivative (0.5 mmol) was resolved in in 3 mL of HF/pyridine/THF (1:1:18, v/v) and stirred for 6 h at room temperature in a plastic falcon tube. After the reaction completion, the remaining fluoride source was quenched with excess ethoxytrimethylsilane (6 mL). The mixture was concentrated in vacuo, and the resultant product was purified with silica-gel flash column chromatography with ethyl acetate/hexane or dichloromethane/methanol conditions to provide the desired ICM derivative product. Yields: 79%, **2e**; 80%, **2j**; 65%, **2k**; 93%, **2l**; 92%, **2m**; 93%, **2o**.

## ■ ASSOCIATED CONTENT

### 📄 Supporting Information

The Supporting Information is available free of charge on the ACS Publications website at DOI: 10.1021/acs.jmedchem.6b00954.

Procedures for synthetic and biological experiments, and spectroscopic data of all new compounds (PDF)  
Molecular formula strings (CSV)

## ■ AUTHOR INFORMATION

### Corresponding Author

\*Phone: +82-2-880-9090. Fax: +82-2-884-4025. E-mail: sbpark@snu.ac.kr.

### ORCID

Wansang Cho: 0000-0002-5262-9543

Seung Bum Park: 0000-0003-1753-1433

### Author Contributions

#W.S. and J.Y.K. equally contributed to this work.

### Notes

The authors declare no competing financial interest.

## ■ ACKNOWLEDGMENTS

This work was supported by the Creative Research Initiative Grant (2014R1A3A2030423) and the Bio & Medical Technology Development Program (2012M3A9C4048780) through the National Research Foundation of Korea (NRF) funded by the Korean Government (Ministry of Science, ICT & Future Planning). W.C. is grateful for the NRF-2016-Fostering Core Leaders of the Future Basic Science Program/Global Ph.D. Fellowship Program (2016H1A2A1908141). J.Y.K. and S.L. are grateful for their fellowship awarded by the BK21 Plus Program.

## ■ ABBREVIATIONS USED

HMGB, high mobility group box protein; TNF- $\alpha$ , tumor necrosis factor-alpha; IL-1 $\beta$ , interleukin-1-beta; IL-6, interleukin-6; ERK, extracellular signal-regulated kinase; JNK, c-jun N-

terminal kinase; p38, p38 MAPK; NF- $\kappa$ B, nuclear factor kappa-light chain enhancer in B cells; PAMP, pathogen associated molecular pattern; PRR, pattern recognition receptor; ICM, inflachromene; EGCG, (–)-epigallocatechin-3-gallate; ELISA, enzyme linked immunosorbent assay; ip, intraperitoneal; PK, pharmacokinetics; CLP, cecal ligation and puncture; Lys, cell lysate; CM, culture medium; LPS, lipopolysaccharide; Cpd, compound

## REFERENCES

- (1) Bone, R. C.; Sibbald, W. J.; Sprung, C. L. The ACCP-SCCM Consensus Conference on Sepsis and Organ Failure. *Chest* **1992**, *101*, 1481–1483.
- (2) Levy, M. M.; Fink, M. P.; Marshall, J. C.; Abraham, E.; Angus, D.; Cook, D.; Cohen, J.; Opal, S. M.; Vincent, J. L.; Ramsay, G. 2001 SCCM/ESICM/ACCP/ATS/SIS International Sepsis Definitions Conference. *Crit. Care Med.* **2003**, *31*, 1250–1256.
- (3) Deutschman, C. S.; Tracey, K. J. Sepsis: Current Dogma and New Perspectives. *Immunity* **2014**, *40*, 463–475.
- (4) Takeuchi, O.; Akira, S. Pattern Recognition Receptors and Inflammation. *Cell* **2010**, *140*, 805–820.
- (5) Mogensen, T. H. Pathogen Recognition and Inflammatory Signaling in Innate Immune Defenses. *Clin. Microbiol. Rev.* **2009**, *22*, 240–273.
- (6) Rittirsch, D.; Flierl, M. A.; Ward, P. A. Harmful Molecular Mechanisms in Sepsis. *Nat. Rev. Immunol.* **2008**, *8*, 776–787.
- (7) Angus, D. C.; van der Poll, T. Severe Sepsis and Septic Shock. *N. Engl. J. Med.* **2013**, *369*, 840–851.
- (8) Angus, D. C.; Linde-Zwirble, W. T.; Lidicker, J.; Clermont, G.; Carcillo, J.; Pinsky, M. R. Epidemiology of Severe Sepsis in the United States: Analysis of Incidence, Outcome, and Associated Costs of Care. *Crit. Care Med.* **2001**, *29*, 1303–1310.
- (9) Rangel-Frausto, M. S.; Pittet, D.; Costigan, M.; Hwang, T.; Davis, C. S.; Wenzel, R. P. The Natural History of the Systemic Inflammatory Response Syndrome (SIRS). *JAMA* **1995**, *273*, 117–123.
- (10) Kaukonen, K.-M.; Bailey, M.; Suzuki, S.; Pilcher, D.; Bellomo, R. Mortality Related to Severe Sepsis and Septic Shock among Critically Ill Patients in Australia and New Zealand, 2000–2012. *JAMA* **2014**, *311*, 1308–1316.
- (11) Torio, C. M.; Andrews, R. M. *National Inpatient Hospital Costs: The Most Expensive Conditions by Payer, 2011*; U.S. Agency for Health Care Policy and Research: Rockville, MD, 2013.
- (12) Fink, M. P.; Warren, H. S. Strategies to Improve Drug Development for Sepsis. *Nat. Rev. Drug Discovery* **2014**, *13*, 741–758.
- (13) Ulloa, L.; Tracey, K. J. The “Cytokine Profile”: A Code for Sepsis. *Trends Mol. Med.* **2005**, *11*, 56–63.
- (14) Ertel, W.; Kremer, J. P.; Kenney, J.; Steckholzer, U.; Jarrar, D.; Trentz, O.; Schildberg, F. W. Downregulation of Proinflammatory Cytokine Release in Whole Blood from Septic Patients. *Blood* **1995**, *85*, 1341–1347.
- (15) Whang, K. T.; Vath, S. D.; Becker, K. L.; Snider, R. H.; Nysten, E. S.; Muller, B.; Li, Q.; Tamarkin, L.; White, J. C. Procalcitonin and Proinflammatory Cytokine Interactions in Sepsis. *Shock* **2000**, *14*, 73–78.
- (16) Bouchon, A.; Facchetti, F.; Weigand, M. A.; Colonna, M. TREM-1 Amplifies Inflammation and Is a Crucial Mediator of Septic Shock. *Nature* **2001**, *410*, 1103–1107.
- (17) Lorente, J. A.; Marshall, J. C. Neutralization of Tumor Necrosis Factor in Preclinical Models of Sepsis. *Shock* **2005**, *24*, 107–119.
- (18) Alexander, H. R.; Doherty, G. M.; Buresh, C. M.; Venzon, D. J.; Norton, J. A. A Recombinant Human Receptor Antagonist to Interleukin 1 Improves Survival after Lethal Endotoxemia in Mice. *J. Exp. Med.* **1991**, *173*, 1029–1032.
- (19) Abraham, E.; Laterre, P.-F.; Garbino, J.; Pingleton, S.; Butler, T.; Dugernier, T.; Margolis, B.; Kudsk, K.; Zimmerli, W.; Anderson, P.; Reynaert, M.; Lew, D.; Lesslauer, W.; Passe, S.; Cooper, P.; Burdeska, A.; Modi, M.; Leighton, A.; Salgo, M.; Van der Auwera, P.; Lenercept Study Group. Lenercept (p55 Tumor Necrosis Factor Receptor Fusion Protein) in Severe Sepsis and Early Septic Shock: A Randomized, Double-Blind, Placebo-Controlled, Multicenter Phase III Trial with 1,342 Patients. *Crit. Care Med.* **2001**, *29*, 503–510.
- (20) Opal, S. M.; Fisher, C. J. J.; Dhainaut, J.-F. A.; Vincent, J.-L.; Brase, R.; Lowry, S. F.; Sadoff, J. C.; Slotman, G. J.; Levy, H.; Balk, R. A.; Shelly, M. P.; Pribble, J. P.; LaBrecque, J. F.; Lookabaugh, J.; Donovan, H.; Dubin, H.; Baughman, R.; Norman, J.; DeMaria, E.; Matzel, K.; Abraham, E.; Seneff, M. Confirmatory Interleukin-1 Receptor Antagonist Trial in Severe Sepsis: A Phase III, Randomized, Doubleblind, Placebo-Controlled, Multicenter Trial. *Crit. Care Med.* **1997**, *25*, 1115–1124.
- (21) Kellum, J. A.; Kong, L.; Fink, M. P.; Weissfeld, L. A.; Yealy, D. M.; Pinsky, M. R.; Fine, J.; Krichevsky, A.; Delude, R. L.; Angus, D. C.; GenIMS Investigators. Understanding the Inflammatory Cytokine Response in Pneumonia and Sepsis: Results of the Genetic and Inflammatory Markers of Sepsis (GenIMS) Study. *Arch. Intern. Med.* **2007**, *167*, 1655–1663.
- (22) Wang, H.; Bloom, O.; Zhang, M.; Vishnubhak, J. M.; Ombrellino, M.; Che, J.; Frazier, A.; Yang, H.; Ivanova, S.; Borovikova, L.; Manogue, K. R.; Faist, E.; Abraham, E.; Andersson, J.; Andersson, U.; Molina, P. E.; Abumrad, N. N.; Sama, A.; Tracey, K. J. HMG-1 as a Late Mediator of Endotoxin Lethality in Mice. *Science* **1999**, *285*, 248–251.
- (23) Lotze, M. T.; Tracey, K. J. High-Mobility Group Box 1 Protein (HMGB1): Nuclear Weapon in the Immune Arsenal. *Nat. Rev. Immunol.* **2005**, *5*, 331–342.
- (24) Yang, H.; Tracey, K. J. Targeting HMGB1 in Inflammation. *Biochim. Biophys. Acta, Gene Regul. Mech.* **2010**, *1799*, 149–156.
- (25) Erlandsson Harris, H.; Andersson, U. Mini-Review: The Nuclear Protein HMGB1 as a Proinflammatory Mediator. *Eur. J. Immunol.* **2004**, *34*, 1503–1512.
- (26) Sims, G. P.; Rowe, D. C.; Rietdijk, S. T.; Herbst, R.; Coyle, A. J. HMGB1 and RAGE in Inflammation and Cancer. *Annu. Rev. Immunol.* **2010**, *28*, 367–388.
- (27) Liu, X.-X.; Wang, C.; Huang, S.-F.; Chen, Q.; Hu, Y.-F.; Zhou, L.; Gu, Y. Regnase-1 in Microglia Negatively Regulates High Mobility Group Box 1-Mediated Inflammation and Neuronal Injury. *Sci. Rep.* **2016**, *6*, 24073.
- (28) Rittirsch, D.; Huber-Lang, M. S.; Flierl, M. A.; Ward, P. A. Immunodesign of Experimental Sepsis by Cecal Ligation and Puncture. *Nat. Protoc.* **2008**, *4*, 31–36.
- (29) Hubbard, W. J.; Choudhry, M.; Schwacha, M. G.; Kerby, J. D.; Rue, L. W.; Bland, K. I.; Chaudry, I. H. Cecal Ligation and Puncture. *Shock* **2005**, *24*, 52–57.
- (30) Yang, H.; Ochani, M.; Li, J.; Qiang, X.; Tanovic, M.; Harris, H. E.; Susarla, S. M.; Ulloa, L.; Wang, H.; DiRaimo, R.; Czura, C. J.; Wang, H.; Roth, J.; Warren, H. S.; Fink, M. P.; Fenton, M. J.; Andersson, U.; Tracey, K. J. Reversing Established Sepsis with Antagonists of Endogenous High-Mobility Group Box 1. *Proc. Natl. Acad. Sci. U. S. A.* **2004**, *101*, 296–301.
- (31) Wang, H.; Liao, H.; Ochani, M.; Justiniani, M.; Lin, X.; Yang, L.; Al-Abed, Y.; Wang, H.; Metz, C.; Miller, E. J.; Tracey, K. J.; Ulloa, L. Cholinergic Agonists Inhibit HMGB1 Release and Improve Survival in Experimental Sepsis. *Nat. Med.* **2004**, *10*, 1216–1221.
- (32) Choi, H. W.; Tian, M.; Song, F.; Venereau, E.; Preti, A.; Park, S.-W.; Hamilton, K.; Swapna, G. V. T.; Manohar, M.; Moreau, M.; Agresti, A.; Gorzanelli, A.; De Marchis, F.; Wang, H.; Antonyak, M.; Micikas, R. J.; Gentile, D. R.; Cerione, R. A.; Schroeder, F. C.; Montelione, G. T.; Bianchi, M. E.; Klessig, D. F. Aspirin’s Active Metabolite Salicylic Acid Targets High Mobility Group Box 1 to Modulate Inflammatory Responses. *Mol. Med.* **2015**, *21*, 526–35.
- (33) Musumeci, D.; Roviello, G. N.; Montesarchio, D. An Overview on HMGB1 Inhibitors as Potential Therapeutic Agents in HMGB1-related Pathologies. *Pharmacol. Ther.* **2014**, *141*, 347–357.
- (34) Wang, H.; Ward, M. F.; Sama, A. E. Targeting HMGB1 in the Treatment of Sepsis. *Expert Opin. Ther. Targets* **2014**, *18*, 257–268.
- (35) Li, W.; Ashok, M.; Li, J.; Yang, H.; Sama, A. E.; Wang, H. A Major Ingredient of Green Tea Rescues Mice from Lethal Sepsis Partly by Inhibiting HMGB1. *PLoS One* **2007**, *2*, e1153.

- (36) Li, W.; Zhu, S.; Li, J.; Assa, A.; Jundoria, A.; Xu, J.; Fan, S.; Eissa, N. T.; Tracey, K. J.; Sama, A. E.; Wang, H. EGCG Stimulates Autophagy and Reduces Cytoplasmic HMGB1 Levels in Endotoxin-Stimulated Macrophages. *Biochem. Pharmacol.* **2011**, *81*, 1152–1163.
- (37) Kim, J.; Kim, H.; Park, S. B. Privileged Structures: Efficient Chemical “navigators” toward Unexplored Biologically Relevant Chemical Spaces. *J. Am. Chem. Soc.* **2014**, *136*, 14629–14638.
- (38) Zhu, M.; Lim, B. J.; Koh, M.; Park, S. B. Construction of Polyheterocyclic Benzopyran Library with Diverse Core Skeletons through Diversity-Oriented Synthesis Pathway: Part II. *ACS Comb. Sci.* **2012**, *14*, 124–134.
- (39) Park, J.; Oh, S.; Park, S. B. Discovery and Target Identification of an Antiproliferative Agent in Live Cells Using Fluorescence Difference in Two-Dimensional Gel Electrophoresis. *Angew. Chem., Int. Ed.* **2012**, *51*, 5447–5451.
- (40) Lee, S.; Nam, Y.; Koo, J. Y.; Lim, D.; Park, J.; Ock, J.; Kim, J.; Suk, K.; Park, S. B. A Small Molecule Binding HMGB1 and HMGB2 Inhibits Microglia-Mediated Neuroinflammation. *Nat. Chem. Biol.* **2014**, *10*, 1055–1060.
- (41) Mosser, D. M.; Edwards, J. P. Exploring the Full Spectrum of Macrophage Activation. *Nat. Rev. Immunol.* **2008**, *8*, 958–969.
- (42) Filiano, A. J.; Gadani, S. P.; Kipnis, J. Interactions of Innate and Adaptive Immunity in Brain Development and Function. *Brain Res.* **2015**, *1617*, 18–27.
- (43) Bonaldi, T.; Talamo, F.; Scaffidi, P.; Bachi, A.; Porto, A.; Rubartelli, A.; Agresti, A.; Bianchi, M. E. Monocytic Cells Hyperacetylate Chromatin Protein HMGB1 to Redirect It towards Secretion. *EMBO J.* **2003**, *22*, 5551–5560.
- (44) Ghosh, M.; Garcia-Castillo, D.; Aguirre, V.; Golshani, R.; Atkins, C. M.; Bramlett, H. M.; Dietrich, W. D.; Pearse, D. D. Proinflammatory Cytokine Regulation of Cyclic AMP-Phosphodiesterase 4 Signaling in Microglia in Vitro and Following CNS Injury. *Glia* **2012**, *60*, 1839–1859.
- (45) Park, B. S.; Song, D. H.; Kim, H. M.; Choi, B.-S.; Lee, H.; Lee, J.-O. The Structural Basis of Lipopolysaccharide Recognition by the TLR4-MD-2 Complex. *Nature* **2009**, *458*, 1191–1195.
- (46) Qiao, S.; Luo, Q.; Zhao, Y.; Zhang, X. C.; Huang, Y. Structural Basis for Lipopolysaccharide Insertion in the Bacterial Outer Membrane. *Nature* **2014**, *511*, 108–111.
- (47) Dong, H.; Xiang, Q.; Gu, Y.; Wang, Z.; Paterson, N. G.; Stansfeld, P. J.; He, C.; Zhang, Y.; Wang, W.; Dong, C. Structural Basis for Outer Membrane Lipopolysaccharide Insertion. *Nature* **2014**, *511*, 52–56.
- (48) Meng, F.; Lowell, C. A. Lipopolysaccharide (LPS)-Induced Macrophage Activation and Signal Transduction in the Absence of Src-Family Kinases Hck, Fgr, and Lyn. *J. Exp. Med.* **1997**, *185*, 1661–1670.
- (49) Hajishengallis, G.; Lambris, J. D. Microbial Manipulation of Receptor Crosstalk in Innate Immunity. *Nat. Rev. Immunol.* **2011**, *11*, 187–200.
- (50) Tsikas, D. Analysis of Nitrite and Nitrate in Biological Fluids by Assays Based on the Griess Reaction: Appraisal of the Griess Reaction in the L-Arginine/nitric Oxide Area of Research. *J. Chromatogr. B: Anal. Technol. Biomed. Life Sci.* **2007**, *851*, 51–70.
- (51) Kawai, T.; Akira, S. Signaling to NF- $\kappa$ B by Toll-like Receptors. *Trends Mol. Med.* **2007**, *13*, 460–469.
- (52) Zhang, W.; Liu, H. T. MAPK Signal Pathways in the Regulation of Cell Proliferation in Mammalian Cells. *Cell Res.* **2002**, *12*, 9–18.
- (53) Rao, K. M. K. MAP Kinase Activation in Macrophages. *J. Leukoc. Biol.* **2001**, *69*, 3–10.
- (54) Oeckinghaus, A.; Hayden, M. S.; Ghosh, S. Crosstalk in NF- $\kappa$ B Signaling Pathways. *Nat. Immunol.* **2011**, *12*, 695–708.
- (55) Avdeef, A.; Berger, C. M.; Brownell, C. pH-Metric Solubility. 2. Correlation Between the Acid-Base Titration and the Saturation Shake-Flask Solubility-pH Methods. *Pharm. Res.* **2000**, *17*, 85–89.
- (56) Chang, C. E.; Gilson, M. K. Tork: Conformational Analysis Method for Molecules and Complexes. *J. Comput. Chem.* **2003**, *24*, 1987–1998.
- (57) Zhu, M.; Kim, M. H.; Lee, S.; Bae, S. J.; Kim, S. H.; Park, S. B. Discovery of Novel Benzopyranyl Tetracycles That Act as Inhibitors of Osteoclastogenesis Induced by Receptor Activator of NF- $\kappa$ B Ligand. *J. Med. Chem.* **2010**, *53*, 8760–8764.